Cramér Rao Lower Bound for Underwater Range Estimation with Noisy Sound Speed Profile

Hamid Ramezani*, Raj Thilak Rajan, *Student Member, IEEE*, Milica Stojanovic, *Fellow, IEEE* and Geert Leus, *Fellow, IEEE*

***Abstract*—In this paper, the Cramér Rao bound (CRB) for range estimate between two underwater nodes is calculated. The nodes are equipped with Conductivity-Temperature-Density (CTD) sensors to measure their depths, and the sound speed at different depths, and an acoustic modem to measure their mutual time of flight. The measurement noise is assumed to be Gaussian distributed. We show how much the CRB gets affected by each measurement noise. For long distances, the effect of sound speed measurement noise is dominant, and its impact depends on the actual sound speed profile, the depths at which the sound speed samples are gathered, and the number of samples.**

I. Introduction

Range estimation is required mostly for sensor network localization, and navigations. In this paper we tackle the problem of Cramér Rao bound (CRB) for range estimation in an underwater medium. The CRB shows how accurate a parameter can be estimated via several measurements. The range estimation CRB for terrestrial environment where sensor nodes communicate with each other through radio frequency has been investigated in [1]. There, the time of flight (ToF) measurement is used for range estimation, and it is shown that the corresponding CRB depends on signal bandwidth, wave propagation speed, and received signal to noise ratio. Apart from range information in the time delay, [2] has reached to a more accurate formulation by extracting the range information in the amplitude of the received signal power. Although, the results of the above papers give us a valid inception of range estimation accuracy in free space, they do not justify why practical underwater range estimation (specifically for long distances) suffer from higher inaccuracy than the bound anticipated by them.

Acoustic underwater communications is quite different from its terrestrial counterparts [3]. The propagation speed is not constant and it varies with temperature, salinity and pressure [4]. On the other hand, the underwater sensor nodes have this privilege to measure their depth via pressure sensor. In [5], it is shown that knowing the depth information, and sound speed profile (SSP), a mutual distance between two nodes can be obtained via single ToF measurement. Under these conditions the CRB for range estimation has been derived for a multiple-isogradient sound speed profile in [5], and for a more general sound speed profile in [6]. However, sound speed profile has to be measured in actual scenarios, and consequently the noisy measurement would indirectly affect the accuracy of the range estimation. The SSP can be represented as a linear combination of N basis functions obtained from empirical data as [7]

$$c(z) = \bar{c}(z) + \sum_{n=1}^{N} a_n f_n(z), \tag{1}$$

where $\bar{c}(z)$ is the mean sound speed profile which is known a priori (obtained from historical data), and $f_n(z)$ for $n = 1, 2, ..., N$ are the basis functions.

In order to measure the sound speed at a certain depth, a CTD sensor is used. Gathering all the measurements at M different depth leads to

$$\mathbf{c} = \bar{\mathbf{c}} + F\mathbf{a} + \mathbf{v}, \tag{2}$$

where $\mathbf{c} = [c(z_1), c(z_2), \ldots, c(z_M)]^T$ is a vector of noisy sound speed samples at different depths, $\bar{\mathbf{c}} = [\bar{c}(z_1), \bar{c}(z_2), \ldots, \bar{c}(z_M)]^T$, $\mathbf{a} = [a_1, a_2, ..., a_N]^T$, F is $M \times N$ matrix where its j-th column ($j = \{1, 2, .., N\}$) is $\mathbf{f}_j = [f_j(z_1), f_j(z_2), \ldots, f_j(z_M)]^T$, and $\mathbf{v}$ is the Gaussian distributed measurement noise with covariance $R_{\mathbf{v}} = \sigma_c^2 I_{M\times M}$.

II. Ray Tracing

The relation between the ToF and the node positions can be extracted from a set of differential equations characterized by Snell's law ,

$$\frac{\cos\theta_{\rm s}}{c(z_{\rm s})} = \frac{\cos\theta_{\rm d}}{c(z_{\rm d})} = \frac{\cos\theta}{c(z)} = k_0, \quad \theta \in \left(-\frac{\pi}{2}, \frac{\pi}{2}\right) \tag{3}$$

where k_0 is constant for a given ray, $\theta_{\rm s}$, and $\theta_{\rm d}$ are the ray angle at the source and the destination, respectively, θ is the ray angle at any point between the source and the destination, and $z_{\rm s}$ and $z_{\rm d}$ are the depths of the source and destination respectively as shown in Fig. 1. The basic relationship between the time of flight t, horizontal distance h, and depth z can be represented by

$$\partial h = \frac{\partial z}{\sin\theta} \tag{4}$$

$$\partial t = \frac{\partial h}{c(z)} \tag{5}$$

which will be used in calculating the ToF and horizontal distance between two points.

†The authors are with the Faculty of Electrical Engineering, Mathematics and Computer Science, Delft University of Technology, 2826 CD Delft, The Netherlands. e-mails: {h.mashhadiramezani, g.j.t.leus}@tudelft.nl.

* Corresponding author: Hamid Ramezani, phone: (+31)152786280, fax: (+31)152786190, e-mail: h.mashhadiramezani@tudelft.nl.

The research leading to these results has received funding in part from the European Commission FP7-ICT Cognitive Systems, Interaction, and Robotics under the contract #270180 (NOPTILUS)

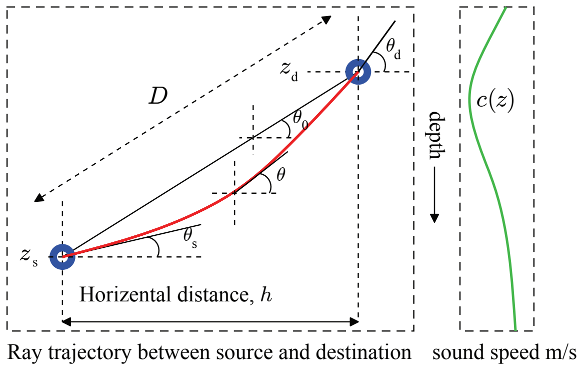

Fig. 1: Ray propagation between the source and destination.

Although, in an underwater medium with general SSP, a ray between two points can have different patterns [5], here we assume that the ray crosses any depth between the two points only once. With this assumption the ToF and the horizontal distance can be formulated as

$$t = \int_{z_s}^{z_d} \frac{1}{c(z)\sqrt{1-[k_0 c(z)]^2}} d_z, \tag{6}$$

$$h = \int_{z_s}^{z_d} \frac{k_0 c(z)}{\sqrt{1-[k_0 c(z)]^2}} d_z. \tag{7}$$

With the knowledge of ToF, SSP, and depths, one can calculate k_0 from (6), and use that in (7) to find the horizontal distance and eventually the range between the two points. Unfortunately, the measurements are always noisy and that makes the estimation inaccurate. In the next section, we investigate what is the lowest bound for the range estimation accuracy.

III. Cramér Rao Lower Bound

As explained before, the measurements are ToF t, depth of the source z_s, depth of the destination z_d, and the samples of the sound speed at different depths $\bar{c}$, each contaminated by respective Gaussian-distributed noise with zero mean and variance σ_t^2, σ_z^2, σ_z^2, and covariance $\sigma_c^2 I_{M\times M}$. Stacking all the measurements in a vector we have

$$\mathbf{f}^T = [t, z_s, z_e, \tilde{\mathbf{c}}^T], \tag{8a}$$

$$\mathbf{w}^T = [\sigma_t^2, \sigma_z^2, \sigma_z^2, \sigma_c^2 \mathbf{1}_{1\times M}], \tag{8b}$$

$$\mathbf{x}^T = [k_0, z_s, z_e, \mathbf{a}^T], \tag{8c}$$

where $\mathbf{f}$ is the measurement vector, $\mathbf{w}$ is the noise power of each measurement (assumed to be independent of each other), and $\mathbf{x}$ is a vector whose elements are the parameters that we are going to estimate. Later, we will show how with simple change of variables, the CRB for horizontal distance and the mutual distance can be obtained. For Gaussian distributed noise, the elements of the Fisher information matrix (FIM) can be obtained as [8]

$$[\mathbf{I_x}]_{i,j} = \frac{\partial \mathbf{f}}{\partial x_i}^T \mathbf{R}_w^{-1} \frac{\partial \mathbf{f}}{\partial x_j} + \frac{1}{2}\mathrm{tr}\left[\mathbf{R}_w^{-1}\frac{\partial \mathbf{R}_w}{\partial x_i}\mathbf{R}_w^{-1}\frac{\partial \mathbf{R}_w}{\partial x_j}\right]. \tag{9}$$

Among the list of the measurements, variance of the ToF is distance dependent [9], and as a result the second term of (9) is not zero for $[\mathbf{I_x}]_{1,1}$, still it can be ignored for high values of SNR. The diagonal element of the inverse of the Fisher information matrix gives us the lowest bound on the variance of an unbiased estimator. The inverse of FIM (which is symmetric) can be calculated as (see Appendix A)

$$\begin{aligned}
[\mathbf{I_x}^{-1}]_{1,1} &= \sigma_t^2 \frac{1}{(\partial t/\partial k_0)^2} + \\
&\quad \sigma_z^2 \frac{(\partial t/\partial z_s)^2}{(\partial t/\partial k_0)^2} + \sigma_z^2 \frac{(\partial t/\partial z_d)^2}{(\partial t/\partial k_0)^2} + \\
&\quad \sigma_c^2 \frac{1}{(\partial t/\partial k_0)^2} \frac{\partial t}{\partial \mathbf{a}^T} \left(F^T F\right)^{-1} \frac{\partial t}{\partial \mathbf{a}}, \\
[\mathbf{I_x}^{-1}]_{1,2} &= -\sigma_z^2 \frac{\partial t/\partial z_s}{\partial t/\partial k_0}, \\
[\mathbf{I_x}^{-1}]_{1,3} &= -\sigma_z^2 \frac{\partial t/\partial z_d}{\partial t/\partial k_0}, \\
[\mathbf{I_x}^{-1}]_{1,4:N+3} &= -\sigma_c^2 \frac{1}{\partial t/\partial k_0} \frac{\partial t}{\partial \mathbf{a^T}} \left(F^T F\right)^{-1}, \\
[\mathbf{I_x}^{-1}]_{2,2} &= \sigma_z^2 \\
[\mathbf{I_x}^{-1}]_{3,3} &= \sigma_z^2 \\
[\mathbf{I_x}^{-1}]_{2:4,4:N+3} &= \mathbf{0} \\
[\mathbf{I_x}^{-1}]_{4:N+3,4:N+3} &= \sigma_c^2 \left(F^T F\right)^{-1},
\end{aligned} \tag{10}$$

where

$$\begin{aligned}
\frac{\partial t}{\partial k_0} &= \int_{z_s}^{z_d} \frac{k_0 c(z)}{(1-[k_0 c(z)]^2)^{\frac{3}{2}}} dz, \\
\frac{\partial t}{\partial z_s} &= \frac{-1}{c(z_s)\sqrt{1-[k_0 c(z_s)]^2}}, \\
\frac{\partial t}{\partial z_d} &= \frac{1}{c(z_d)\sqrt{1-[k_0 c(z_d)]^2}},
\end{aligned}$$

and $\frac{\partial t}{\partial \mathbf{a}}$ is a $N \times 1$ vector $[\frac{\partial t}{\partial a_1}, \frac{\partial t}{\partial a_2}, ..., \frac{\partial t}{\partial a_N}]^T$ including the derivatives of the ToF to the coefficients of the basis functions in (1) and can be obtained as

$$\frac{\partial t}{\partial a_n} = \int_{z_s}^{z_d} \frac{2[k_0 c(z)]^2 - 1}{c^2(z)(1-[k_0 c(z)]^2)^{\frac{3}{2}}} f_n(z) dz$$

In order to calculate the CRB for the horizontal distance we use change of variable $\mathbf{y}^T = [h, z_s, z_d, \mathbf{a}^T]$ similar to [6], and consequently the inverse of the FIM of $\mathbf{y}$ can be obtained from that of $\mathbf{x}$ as

$$\mathbf{I_y}^{-1} = H^T \mathbf{I_x}^{-1} H, \tag{11}$$

where H is the Jacobian matrix of $\mathbf{y}$ with respect to the $\mathbf{x}$ and can be formulated as

$$H = \begin{bmatrix} \frac{\partial h}{\partial k_0} & \frac{\partial h}{\partial z_s} & \frac{\partial h}{\partial z_d} & \frac{\partial h}{\partial \mathbf{a}^T} \\ \mathbf{0}_{N+2\times 1} & & \mathbf{I}_{N+2\times N+2} & \end{bmatrix}^T, \tag{12}$$

where

$$\frac{\partial h}{\partial k_0} = \frac{1}{k_0}\frac{\partial t}{\partial k_0},$$
$$\frac{\partial h}{\partial z_s} = k_0 c^2(z_s)\frac{\partial t}{\partial z_s},$$
$$\frac{\partial h}{\partial z_d} = k_0 c^2(z_d)\frac{\partial t}{\partial z_d},$$
$$\frac{\partial h}{\partial a_n} = \int_{z_s}^{z_d} \frac{k_0}{(1-[k_0 c(z)]^2)^{\frac{3}{2}}} f_n(z)dz \tag{13}$$

and $\mathbf{I}$ is the identity matrix. Using (12) in (11), and taking the $[\mathbf{I}_{\mathbf{y}}^{-1}]_{11}$ as the CRB of h would be

$$\begin{aligned}\mathrm{CRB}_h =& \sigma_t^2 \frac{1}{k_0^2} + \\ & \sigma_z^2 \frac{1-[k_0 c(z_s)]^2}{[k_0 c(z_s)]^2} + \sigma_z^2 \frac{1-[k_0 c(z_d e)]^2}{[k_0 c(_d)]^2} + \\ & \sigma_c^2 \|\frac{\partial h}{\partial \mathbf{a}} - \frac{1}{k_0}\frac{\partial t}{\partial \mathbf{a}}\|^2_{(F^T F)^{-1}}\end{aligned} \tag{14}$$

where $\|\mathbf{x}\|_A^2 = \mathbf{x}^T A \mathbf{x}$, and $\frac{\partial h}{\partial \mathbf{a}} - \frac{1}{k_0}\frac{\partial t}{\partial \mathbf{a}}$ can be considered as the inner product of $g(z)$ and the basis functions for $z \in [z_s, z_d]$ where

$$g(z) = \frac{1}{k_0 c^2(z)\sqrt{1-[k_0 c(z)]^2}}. \tag{15}$$

In 3D underwater localization [10], it is shown that only the horizontal distance between the each pair of nodes can be used for self-localization.

Using similar procedure as explained above for range (denoted by D) estimation as a function of h, z_s, and z_d, i.e., $D = \sqrt{h^2 + (z_s - z_d)^2}$, the CRB of range estimation can be formulated as

$$\mathrm{CRB}_D = \mathbf{G}^T [\mathbf{I}_{\mathbf{y}}^{-1}]_{1:3,1:3}\mathbf{G}, \tag{16}$$

where $\mathbf{G} = \partial D / \partial [h, z_s, z_d]^T = [\cos\theta_0 \quad -\sin\theta_0 \quad \sin\theta_0]^T$, and θ_0 is the angle between the straight line from the source to the destination and the horizontal axis. The CRB of D can be simplified as

$$\begin{aligned}\mathrm{CRB}_D =& \sigma_t^2 c(z_s)^2 \left(\frac{\cos\theta_0}{\cos\theta_s}\right)^2 + \\ & \sigma_z^2 \left(\frac{\sin[\theta_0 - \theta_s]}{\cos\theta_s}\right)^2 + \sigma_z^2 \left(\frac{\sin[\theta_0 - \theta_d]}{\cos\theta_d}\right)^2 + \\ & \sigma_c^2 (\cos\theta_0)^2 \|\frac{\partial h}{\partial \mathbf{a}} - \frac{1}{k_0}\frac{\partial t}{\partial \mathbf{a}}\|^2_{(F^T F)^{-1}}.\end{aligned} \tag{17}$$

Regarding noisy sound speed samples, it can be observed that five factors affect the CRB, measurement noise power, how the ray propagates (the actual sound speed profile), number of samples M, the depth at which the samples are taken, and the inner product of $g(z)$ with the truncated form of basis functions. It can be proven that if we have a set of basis functions within depths $[z_s, z_d]$ that $g(z)$ can be expanded without any residual, then the third term in (17) is independent of the basis functions for large sound speed samples obtained linearly at $[z_s, z_d]$, however the upper-bounded is

$$\|\frac{\partial h}{\partial \mathbf{a}} - \frac{1}{k_0}\frac{\partial t}{\partial \mathbf{a}}\|^2_{(F^T F)^{-1}} \leq \frac{|z_d - z_s|}{M}\int_{z_s}^{z_d} g^2(z)dz. \tag{18}$$

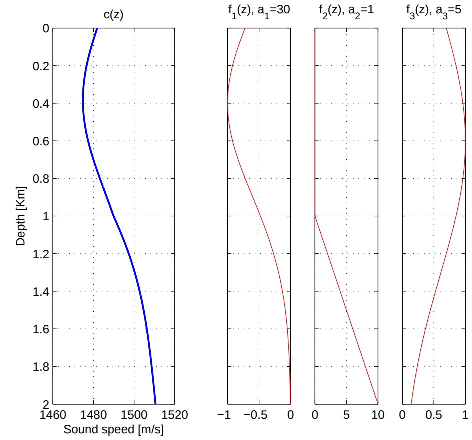

Fig. 2: The sound speed profile as a function of depth, and the basis functions.

The effects of noisy depth and ToF measurements on range estimation have been analyzed before in [6] and [5] for known SSP. In the numerical section we focus more on the effect of noisy sound speed samples.

IV. Numerical Results

In this section we evaluate the CRB of the range estimation for a given set up. A 2D environment with length $D_h = 10$Km and depth $D_z = 2$Km is considered. The average sound speed is set to $\bar{c}(z) = 1500$m/s, and it is assumed that the SSP is composed of three basis functions as depicted in Fig. 2. The depth of the source node is set to $z_s = 0$, and the coordinate of the destination point $[h, z_d]$ varies over the area that the direct path between the source and the destination exists. In addition, there are $M = 10$ sound speed samples obtained at $z_m = m\frac{D_z}{M}$ for $m = \{1, 2, ..., M\}$. The variance of the measurements are $\sigma_t^2 = 10^{-8}$, $\sigma_z^2 = 1$, and $\sigma_c^2 = 1$.

Fig. 3 illustrates the effect of each phenomenon on the CRB of D in part a, b, and c for the normalized noise power, and the overall CRB for D in part d. The white areas in these figures indicate that there is not any direct path between the source and the destination there (shadow zones). It can be observed that for long distances the noisy ToF measurement deteriorates the performance almost similarly for any position of the destination point, and for small ToF measurement noise power, its effect is trivial. Furthermore, the depth measurement error is not effective in the CRB for actual values of noise power (e.g., $\sigma_z = 1$). In contrast, the effect of noisy SSP is dominant here, and it is more dominant when the vertical distance between the source and destination is much lower than the horizontal distance.

V. Conclusions

The CRB of the range estimation in an underwater sensor network with depth-dependent sound-speed where noisy time of flight, depth, and sound speed measurements are available, has been considered in this paper. The effect of each measurement noise on the CRB of range estimation has been evaluated analytically. For long distances the noise power of depth measurements does not play a significant role in the CRB, while those of ToF and sound speed samples are dominant. In long distances even with perfect ToF measurement the range estimation cannot be perfect. It has been shown that for few sound speed samples at different depth several factors such as the basis functions that the sound speed profile (SSP) is composed of, the actual SSP, the number of sound speed samples, and the positions of the source and the destination play a role in the CRB.

VI. APPENDIX

The Fisher information matrix can be represented as

$$\mathbf{I_x} = \begin{bmatrix} A & B \\ B^T & D \end{bmatrix} \quad (19)$$

where

$$\begin{aligned} A =& \frac{1}{\sigma_t^2} \begin{bmatrix} \frac{\partial t}{\partial k_0} \\ \frac{\partial t}{\partial z_s} \\ \frac{\partial t}{\partial z_e} \end{bmatrix} \begin{bmatrix} \frac{\partial t}{\partial k_0} & \frac{\partial t}{\partial z_s} & \frac{\partial t}{\partial z_e} \end{bmatrix} + \frac{1}{\sigma_z^2} \begin{bmatrix} 0 & 0 & 0 \\ 0 & 1 & 0 \\ 0 & 0 & 1 \end{bmatrix}, \\ B =& \frac{1}{\sigma_t^2} \begin{bmatrix} \frac{\partial t}{\partial k_0} \\ \frac{\partial t}{\partial z_s} \\ \frac{\partial t}{\partial z_e} \end{bmatrix} \frac{\partial t}{\partial \mathbf{a}^T}, \\ D =& \frac{1}{\sigma_t^2} \frac{\partial t}{\partial \mathbf{a}} \frac{\partial t}{\partial \mathbf{a}^T} + \frac{1}{\sigma_c^2} F^T F. \end{aligned} \quad (20)$$

Using the general formula of matrix inversion in block form, the inverse FIM in (19) can be obtained as

$$\begin{aligned} &\left[\mathbf{I_x^{-1}}\right] = \\ &\begin{bmatrix} (A - BD^{-1}B^T)^{-1} & -A^{-1}B(D - B^T A^{-1})^{-1} \\ -(D - B^T A^{-1})^{-1} B^T A^{-1} & (D - B^T A^{-1})^{-1} \end{bmatrix}. \end{aligned} \quad (21)$$

The first block of (21) can be further expanded according to the Woodbury identity as [11]

$$\begin{aligned} &(A - BD^{-1}B^T)^{-1} = \\ &\qquad A^{-1} + A^{-1}B(D - B^T A^{-1}B)^{-1} B^T A^{-1}, \end{aligned} \quad (22)$$

which makes the analytical calculation easier. The matrix A is a 3×3 symmetric positive definite matrix and it can be shown that the elements of the A^{-1} are

$$\begin{aligned} [A^{-1}]_{11} =& \frac{\sigma_t^2}{(\partial t/\partial k_0)^2} + \sigma_z^2 \frac{(\partial t/\partial z_\mathrm{s})^2}{(\partial t/\partial k_0)^2} + \sigma_z^2 \frac{(\partial t/\partial z_\mathrm{d})^2}{(\partial t/\partial k_0)^2} \\ [A^{-1}]_{12} =& -\sigma_z^2 \frac{\partial t/\partial z_\mathrm{s}}{\partial t/\partial k_0} \\ [A^{-1}]_{13} =& -\sigma_z^2 \frac{\partial t/\partial z_\mathrm{d}}{\partial t/\partial k_0} \\ [A^{-1}]_{23} =& 0, \\ [A^{-1}]_{22} =& \sigma_z^2. \end{aligned} \quad (23)$$

Using (23) in $A^{-1}B$ leads to

$$\begin{aligned} A^{-1}B &= \begin{bmatrix} \frac{1}{\partial t/\partial k_0} \\ 0 \\ 0 \end{bmatrix} \frac{\partial t}{\partial \mathbf{a^T}} \\ B^T A^{-1} B &= \frac{1}{\sigma_t^2} \frac{\partial t}{\partial \mathbf{a}} \frac{\partial t}{\partial \mathbf{a^T}}, \end{aligned} \quad (24)$$

therefore the second term of (22) is

$$\begin{aligned} &A^{-1}B(D - B^T A^{-1}B)^{-1} B^T A^{-1} = \\ &\frac{1}{(\partial t/\partial k_0)^2} \begin{bmatrix} \frac{\partial t}{\partial \mathbf{a}^T} \left(\frac{1}{\sigma_c^2} F^T F\right)^{-1} \frac{\partial t}{\partial \mathbf{a}} & 0 & 0 \\ 0 & 0 & 0 \\ 0 & 0 & 0 \end{bmatrix}, \end{aligned} \quad (25)$$

which means that the second term of (22) only affects the lower bound of the variance of k_0 estimator. Using similar approach for other matrix blocks in (21) leads to (10).

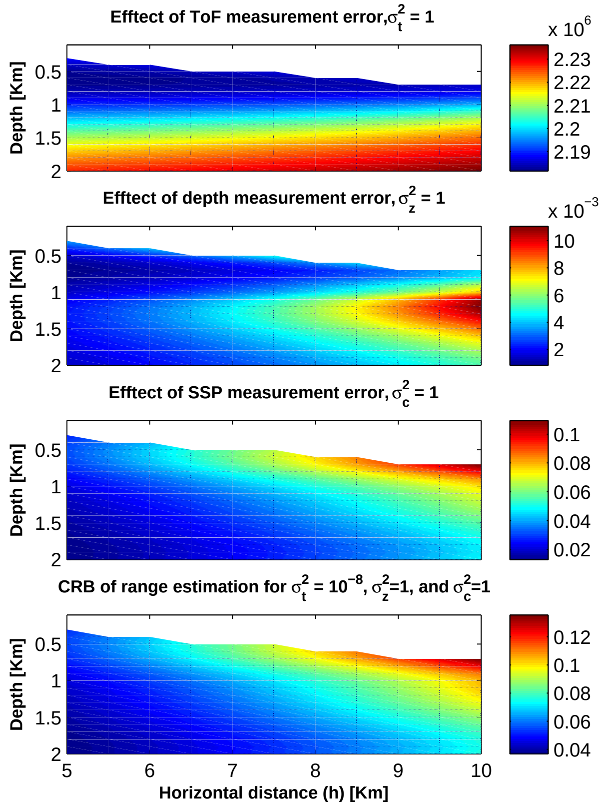

Fig. 3: CRB of range estimation, a) effect of noisy ToF measurement, b) effect of noisy depth measurement, c) effect of noisy sound speed sample, d) the overall CRB of range estimation.

REFERENCES

[1] R. Cardinali, L. De Nardis, M. Di Benedetto, and P. Lombardo, "Uwb ranging accuracy in high-and low-data-rate applications," *Microwave Theory and Techniques, IEEE Transactions on*, vol. 54, no. 4, pp. 1865–1875, 2006.

[2] Y. Wang, G. Leus, and A.-J. van der Veen, "Cramer-rao bound for range estimation," in *Acoustics, Speech and Signal Processing, 2009. ICASSP 2009. IEEE International Conference on*. IEEE, 2009, pp. 3301–3304.

[3] M. Stojanovic and J. Preisig, "Underwater acoustic communication channels: Propagation models and statistical characterization," *Communications Magazine, IEEE*, vol. 47, no. 1, pp. 84–89, 2009.

[4] A. B. Coppens, "Simple equations for the speed of sound in neptunian waters," *The Journal of the Acoustical Society of America*, vol. 69, no. 3, pp. 862–863, 1981.

[5] H. Ramezani and G. Leus, "Ranging in an underwater medium with multiple isogradient sound speed profile layers," *Sensors*, vol. 12, no. 3, pp. 2996–3017, 2012.

[6] C. R. Berger, S. Zhou, P. Willett, and L. Liu, "Stratification effect compensation for improved underwater acoustic ranging," *Signal Processing, IEEE Transactions on*, vol. 56, no. 8, pp. 3779–3783, 2008.

[7] O. Carriere, J.-P. Hermand, M. Meyer, and J. Candy, "Dynamic estimation of the sound-speed profile from broadband acoustic measurements," in *OCEANS 2007-Europe*. IEEE, 2007, pp. 1–6.

[8] S. M. Kay, "Fundamentals of statistical signal processing: detection theory," 1998.

[9] H. Ramezani, H. Jamali-Rad, and G. Leus, "Target localization and tracking for an isogradient sound speed profile," *Signal Processing, IEEE Transactions on*, vol. 61, no. 6, pp. 1434–1446, 2013.

[10] M. T. Isik and O. B. Akan, "A three dimensional localization algorithm for underwater acoustic sensor networks," *Wireless Communications, IEEE Transactions on*, vol. 8, no. 9, pp. 4457–4463, 2009.

[11] G. H. Golub and C. F. Van Loan, *Matrix computations*. JHU Press, 2012, vol. 3.

VII. APPENDIX II

Assume we have matrix E such that

$$[E]_{ij} = f_i(z).f_j(z) = \int_{z_s}^{z_d} f_i(z)f_j(z)dz, \tag{26}$$

and lets define G as

$$G = \begin{bmatrix} f_1(z_s+0\Delta z) & f_2(z_s+0\Delta z) & ... & f_N(z_s+0\Delta z) \\ \vdots & \vdots & ... & \vdots \\ f_1(z_s+n\Delta z) & f_2(z_s+n\Delta z) & ... & f_N(z_s+n\Delta z) \\ \vdots & \vdots & ... & \vdots \\ f_1(z_s+K\Delta z) & f_2(z_s+K\Delta z) & ... & f_N(z_s+K\Delta z) \end{bmatrix} \tag{27}$$

where $z_2 = z_s + K\Delta z$. Therefor, the matrix E can be obtained as

$$E = \lim_{\Delta z \to 0} \Delta_z G^T G, \tag{28}$$

and for large M, and linear SSP sampling within $[z_s, z_d]$, the matrix E can be approximated as

$$E \approx \frac{z_d - z_s}{M} F^T F. \tag{29}$$

If we have $\Delta z G^T G^{-1} = JJ^T$ where J is a $N \times N$ matrix, then the columns of GJ are orthonormal. Given a function $g(z)$ and a vector $\mathbf{g} = [g(z_s+0\Delta z), ..., g(z_s+K\Delta z)]^T$ we have

$$\|\frac{\partial h}{\partial \mathbf{a}} - \frac{1}{k_0}\frac{\partial t}{\partial \mathbf{a}}\|^2_{(F^TF)^{-1}} = \lim_{\Delta z \to 0} \left(\Delta z(\mathbf{g}^T G)(F^T F)^{-1}(G^T \mathbf{g})\Delta z\right) \tag{30}$$

which for large M and linear sampling can be approximated by

$$\lim_{\Delta z \to 0} \left(\Delta z(\mathbf{g}^T G)(\frac{z_d - z_s}{M}\Delta z G^T G)^{-1}(G^T \mathbf{g})\Delta z\right) \tag{31}$$

where $\lim_{\Delta z \to 0} \Delta z \mathbf{g}^T GJ$ is the expansion of $g(z)$ over the N orthogonal functions. And if $g(z)$ can be represented completely by these orthogonal function then (30) can be approximated by

$$\|\frac{\partial h}{\partial \mathbf{a}} - \frac{1}{k_0}\frac{\partial t}{\partial \mathbf{a}}\|^2_{(F^TF)^{-1}} \approx \frac{|z_d - z_s|}{M} \int_{z_s}^{z_d} g(z).g(z)dz. \tag{32}$$